Physica B 632 (2022) 413733

Contents lists available at ScienceDirect

Physica B: Physics of Condensed Matter

journal homepage: www.elsevier.com/locate/physb

Study of training effect by Kerr microscopy measurement in Fe thin film implanted with F-ions

Sagar Sen [a,b], Ajay Gupta [c], V.R. Reddy [d], Ratnesh Gupta [a,*]

[a] School of Instrumentation, Devi Ahilya Vishwavidyalaya, Khandwa Road, Indore, 452017, India
[b] Department of Physics, Maharaja Bhoj Government P.G. College, Dhar, 454001, India
[c] Physics Department, University of Petroleum and Energy Studies, Dehradun, India
[d] UGC DAE CSR Indore Centre, Khandwa Road, Indore, 452017, India

ARTICLE INFO

Keywords:
Exchange bias
Training effect
Kerr microscopy
Ion implantation
Magnetic ordering

ABSTRACT

The training effect and the evolution of magnetic domain during the magnetization irreversible process of Fe thin film which exhibits exchange bias after F-ion implantation have been studied. Kerr microscopy measurements were carried out at different temperatures of the exchange bias F-implanted Fe thin film after the field-cooling from room temperature. With increasing anti-ferromagnetic (AFM) FeF_2 layer thickness, the value of exchange bias increases and the training effect becomes weaker. Temperature-dependent study of exchange bias field indicates that with increasing F-ion fluences the disorder decreases at the Fe/FeF_2 interface. Specimen of higher ion-fluence indicates a behavior that is changing from non-equilibrium state to equilibrium state and behavior of training effect is suggesting step-like.

1. Introduction

Exchange bias (EB) phenomena was discovered in 1956 and since then EB is studied in many systems to explore theoretical and experimental analysis to use this phenomenon in various magnetic applications [1]. Exchange bias field is the shifting of hysteresis loop along the magnetic field axis when ferromagnetic (FM) and anti-ferromagnetic (AFM) layers are coupled and field cooled below the Néel temperature of AFM [1]. EB effect has potential applications in devices like giant magneto-resistance, tunnel Magneto-resistance, magnetic sensors, spin-valve devices and electrically controllable spin-polarized currents [2–5]. To understand the effect of FM-AFM interface on the EB, several experiments have been performed. The experimental observation of EB phenomena has been understood by different theoretical models: Meiklejohn-Bean model, Malozemoff random field model, domain state model, Mauri model, spin glass model, etc [6–8]. An important feature of EB is the training effect, in which one can observe a decrease of EB field value as a function of the repeated number of hysteresis loops (n) measured at the same temperature in similar conditions. Aging phenomena of exchange bias determines the stability of the exchange bias that is known by the training effect. It is inversely dependent on FM layer thickness and interface structure, etc [9–11]. The effect has attracted scientists equally from the experimental and theoretical points of view. Radu et al. observed the magnetic reversible by polarized neutron reflectivity in Co/CoO while studying the training effect [12]. They observed that the change in the value of H_{EB} with increasing n, is very well fitted with the power law. However, in some cases the value of H_{EB} at $n = 1$ is not reproducible using power-law particularly when higher value of H_{EB} has been observed in the hysteresis loop measurement [13]. This phenomenon is known as thermal and athermal training effects [13–16]. Thermal training effect comes into the picture when thermally activated continuing relaxation of frozen AFM moments has occurred in every hysteresis loop which follows the power-law variation for $n > 1$. Athermal training effect arises because of the reorientation of the AFM interface layer, which is in a metastable state. The metastable state arises due to the field cooling of the specimen [17–19]. Ion implantation is a suitable technique to tailor the properties of a thin film in the desired manner. By controlling ion species, its energy and the fluence, one can achieve the desired variation. Hence, it has been utilized for a variety of phenomena such as erosion, radiation damage, surface/interface mixing etc [20–22].

In the present work, the magnetization reversible process and the training effect of Fe thin film after F-ion implantation with different fluencies have been investigated by observing the change in the FM layer domain image as a function of successive M − H hysteresis loop measurements using Kerr microscopy. F implantation converts a thin layer in

* Corresponding author.
E-mail address: gratnesh_ioi@yahoo.com (R. Gupta).

https://doi.org/10.1016/j.physb.2022.413733
Received 1 November 2021; Received in revised form 12 January 2022; Accepted 1 February 2022
Available online 3 February 2022

the center of Fe layer into FeF_2 which is antiferromagnetic at room temperature. Fe(FM)/FeF_2(AFM) is a well known system to understand the EB phenomenon and it is an ideal system to understand the aging effect.

2. Experimental details

The Al(2 nm)/Fe(30 nm)/Fe^{57}(10 nm)/Fe(30 nm)/substrate film was deposited using ion-beam sputtering technique on Si (100) substrates. Al on the top of the surface has been used as a protective layer. Ultrasonic cleaning with acetone has been used to clean the Si (100) substrates before deposition. For the sputtering, the Argon ion beam has been used and the deposition rate was 3 nm/min. Before deposition of the film, the vacuum in the chamber was 1.6×10^{-6} mBar. In order to form an iron fluoride layer in the center of the iron layer, different pieces of the film were implanted with 35 keV Fluorine ions with two different ion fluences, 5×10^{16} ions/cm^2 and 1×10^{17} ions/cm^2. It has been performed using IONAS accelerator, University of Gottingen, Germany. We have chosen this ion energy so that the maximum ions are deposited at the center to form FeF_2 at the middle of the film [23] to achieve FM/AFM/FM structure. The longitudinal magneto-optical Kerr effect (MOKE) measurements have been done at room temperature. The EB behavior and magnetic domain structure have been obtained in the temperature range from 300 to 10 K by MOKE microscope (M/s Evico Magnetics, Germany). The M − H hysteresis loops have been obtained simultaneously by deriving the magnetization signal from the average domain image intensity.

3. Results and discussion

Grazing incident X-ray diffraction (GIXRD) measurements have been performed to get structure phase information of the thin film before and after ion implantation. Fe layer is in nanocrystalline bcc phase. After F^+ ion implantation, the crystalline size is reduced. (XRD data not shown).

(i) Training effect studies

To understand the training behavior of the implanted films, two samples in which we have observed maximum EB namely 5×10^{16} ions/cm^2 and 1×10^{17} ions/cm^2, were field cooled to 50 K from room temperature in presence of the magnetic field of ±100 mT. To freeze the FM spins, the magnetic field has been applied along the easy axis of magnetization of the FM layer. Fig. 1(a,c) gives the M − H data of 5×10^{16} F-ions/cm^2 and 1×10^{17} F-ions/cm^2 specimens measured at 50 K after field cooling. The observed H_{EB} as a function of loop cycle number (n) along with hysteresis loops is depicted in Fig. 1(b,d) for both the specimens. The change in the value of H_{EB} with the loop number of irradiated films has been fitted by the empirical power law [15]:

$$H_{EB}(n) = H_{EB}(\infty) + \frac{\alpha}{n^{1/2}} \quad (1)$$

where α is an experimental constant and from the fitting, we obtained the value of $H_{EB}(\infty)$. The fit of the experimental H_{EB} value as a function of a number of loops with the above eq. (1) have been given in Fig. 1. Perusal of Fig. 1 suggests that the power-law satisfies very well if the n >

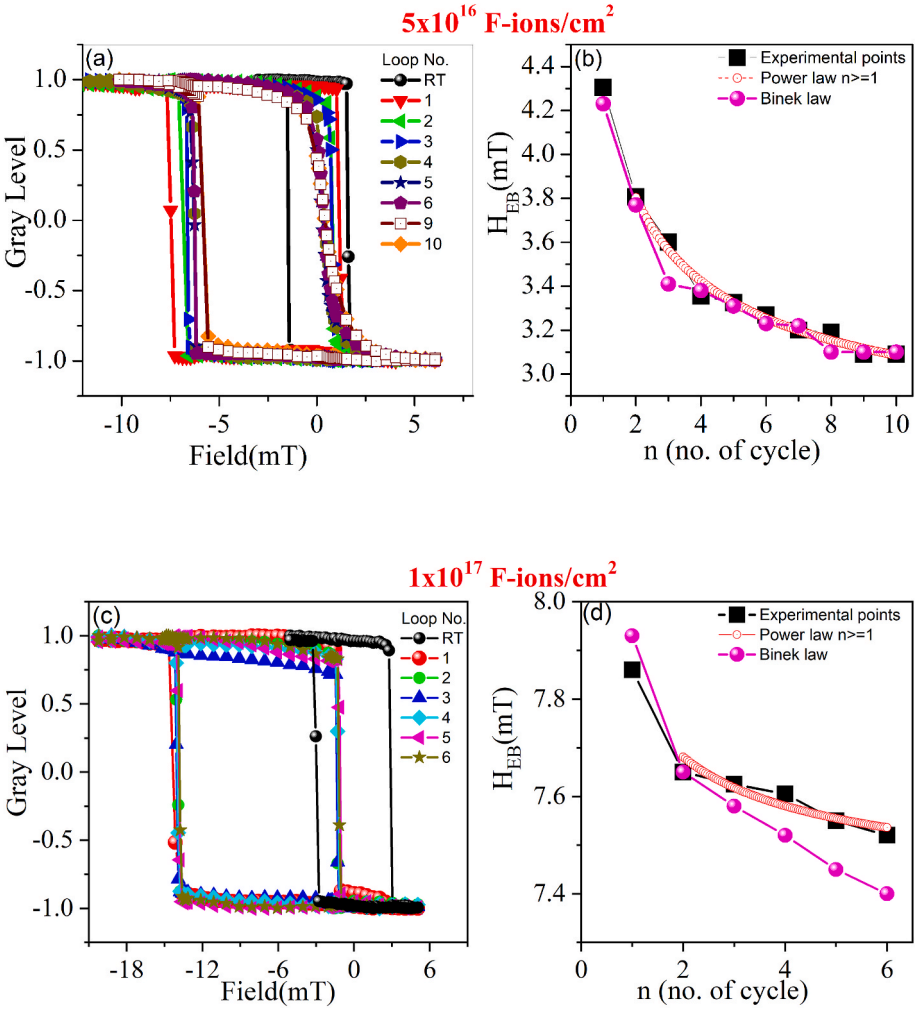

Fig. 1. The hysteresis loops with different cycles and corresponding variation H_{EX} versus n fitted with different models.

1 for both the ion irradiated specimens.

To get a deeper explanation about the training behavior, the H_{EB} behavior has been fitted by the Binek model [13] given by the following relation:

$$H_{EB}(n+1) - H_{EB}(n) = -\gamma[H_{EB}(n) - H_{EB}(\infty)]^3 \quad (2)$$

where $H_{EB}(\infty)$ and γ are the two fitting parameters. The steepness parameter (C) and characteristic decay rate γ can be defined as the following:

$$C = \frac{H_{EB}(n=1) - H_{EB}(n=2)}{H_{EB}(n=1) - H_{EB}(\infty)} \quad (3)$$

$$\gamma = \frac{C}{[H_{EB}(\mathrm{n}=1) - H_{EB}(\infty)]^2} \quad (4)$$

From the fitted graph shown in Fig. 1 clearly suggest that the data including n = 1 has been comparatively better fitted with Binek model. The values of the fitted parameters are shown in Table 1.

The fitted values of C and γ give indication about the training behavior of the exchange bias film. A large value of γ implies that the deviation from the equilibrium state to the non-equilibrium state are higher and vice versa. In addition, the increasing value of C with ion fluence (from Table 1) indicates that the strength of the training effect becomes weaker. Usually, C = 1 resembles step-like behavior, while the obtained value of C < 1 causes to show gradual behavior of H_{EB} versus *n*. The value of C is increasing as a function of ion fluence indicating the gradual behavior of H_{EB} versus *n* change into step-like behavior for 1 × 10^{17} ions/cm^2.

Perusal of Fig. 1 indicates that the relative EB training [(H^1_{EX}- H^6_{EX})/H^1_{EX}] × 100(%) is largest for the sample implanted with 5 × 10^{16} ions/cm^2. It suggests that the spins in the less well-structured formed FeF_2 (i.e., stoichiometric and non-stoichiometric) are more prone to reorientation by the applied field during hysteresis cycle [24,25].

(II) Magnetic domain studies

We have measured the hysteresis loop of the as-deposited thin film in longitudinal mode at room temperature and 9 K in presence of the applied in-plane magnetic field of 100 mT. Fig. 2 displays symmetric M − H loop along with the corresponding Kerr images at specified places of the as-deposited specimen. When the sample is saturated (−10 mT) beyond the coercive field all spins are aligned in the direction of the field and it is represented by white contrast (see image A). On decreasing the field in the opposite direction at point B in the hysteresis loop, the spins begin to reverse the domains by 180° symbolized by black contrast in image (B). While decreasing the field in the opposite direction reverses the domain by 180° completely as shown in images C and D. Image D (in Fig. 2) gives only black contrast which suggests that all spins are saturated in the negative field direction. Similar behavior has been observed in the reverse cycle from images E to A.

Fig. 3 shows the magnetic domain structure obtained at 50 K of ion-irradiated specimens close to the coercive field of ascending and descending branches of M − H loop for increasing values of *n*. The hysteresis loops of both the ion-irradiated specimens are symmetric for *n = 1* and domain structure are also the same for the specimens with the ion fluence of 5 × 10^{16} ions/cm^2 and 1 × 10^{17} ions/cm^2. While the domain structure of higher value of *n* is entirely different for 5 × 10^{16} ions/cm^2 sample. From Fig. 3(a), one can observe that for the nucleated FM domains, the contrast of the domain has been increased with increasing *n* for 5 × 10^{16}ions/cm^2 sample. The domain structure of the 5 × 10^{16} ions/cm^2 sample is different along the descending and ascending branches and it clearly reflects in the corresponding hysteresis loops. For the 1 × 10^{17}ions/cm^2 sample, the domain structure is the same along both the branches (Fig. 3(b)). Usually, the initial loop would be asymmetric and with training effect, the loop becomes symmetric [26]. But in our case, we have observed different results for 5 × 10^{16} ions/cm^2 sample, which may be due to the inhomogeneous formation of FeF_2.

Table 1
Fitting parameter obtained from the eq^n(1) and (2) for 5 × 10^{16} ions/cm^2 and 1 × 10^{17} ions/cm^2 samples.

Sample	$H_{EB}(\infty)$ (mT)	γ (mT^{-2})	C
5 × 10^{16} F- ions/cm^2	2.50	1.21	0.277
1 × 10^{17} F-ions/cm^2	7.33	8.3 × 10^{-2}	0.467

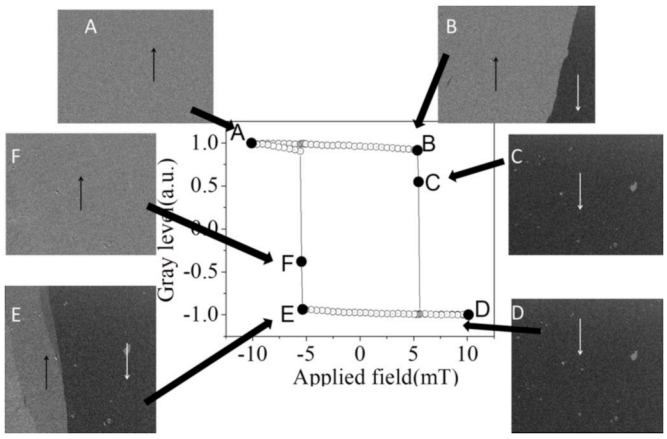

Fig. 2. Longitudinal MOKE hysteresis loop of the as-deposited film with corresponding domain image collected at indicated points from A-F on hysteresis loop. The arrow shows the direction of magnetization.

(III) Temperature-dependent studies

Fig. 4 shows the variation of exchange bias with increasing temperature for 5 × 10^{16} and 1 × 10^{17} ions/cm^2 samples after field cooling. Perusal of Fig. 4, suggests that the behavior of both the films are identical while the magnitude of exchange bias is higher in the case of 1 × 10^{17} ions/cm^2 due to higher degree of homogeneity in the formation of FeF_2. For both the specimens, exchange bias exists up to 70 K, which is very close to the Néel temperature of FeF_2(T_N = 78 K), it suggests that anti-ferromagnetic anisotropy is responsible for the development of exchange bias in the film. The value of H_{EB} is increasing with decreasing temperature, it is due to strong coupling among most of the interfacial spins, which leads to increase in the value of the exchange anisotropy.

Fig. 5 gives the temperature-dependent M − H hysteresis curve for the 5 × 10^{16} ions/cm^2 and 1 × 10^{17} ions/cm^2 specimens and corresponding temperature variation of normalized [H_{EB}(T)/H_{EB}(T = 10 K)]. The temperature-dependent H_{EB}(T) has been fitted with the Malozemoff model with improved correction of exponent [27].

$$H_{EB}(T) \Big/ H_{EB}(T=10K) = B\left(1 - \frac{T}{T_B}\right)^{\nu} \quad (5)$$

where B is a fitting constant, T_B is blocking temperature and exponent ν will provide the information about the magnetic ordering of the AFM layer [8].

The fitted values of the constant B and the exponent (ν) are given in Table 2. The exponent value (ν) is close to unity indicates that the cubic anisotropy of the AFM layer is present in the specimens and its variation from the unity clearly suggests that the disorder is present in the AFM layer [28].

The obtained values of T_B for the two samples are close to 70 K. The exponent value (ν) close to unity indicates the cubic anisotropy of the AFM layer and its deviation from the value of unity suggests that the disorder of the AFM layer is more [28]. The fitted values of exponent (ν)

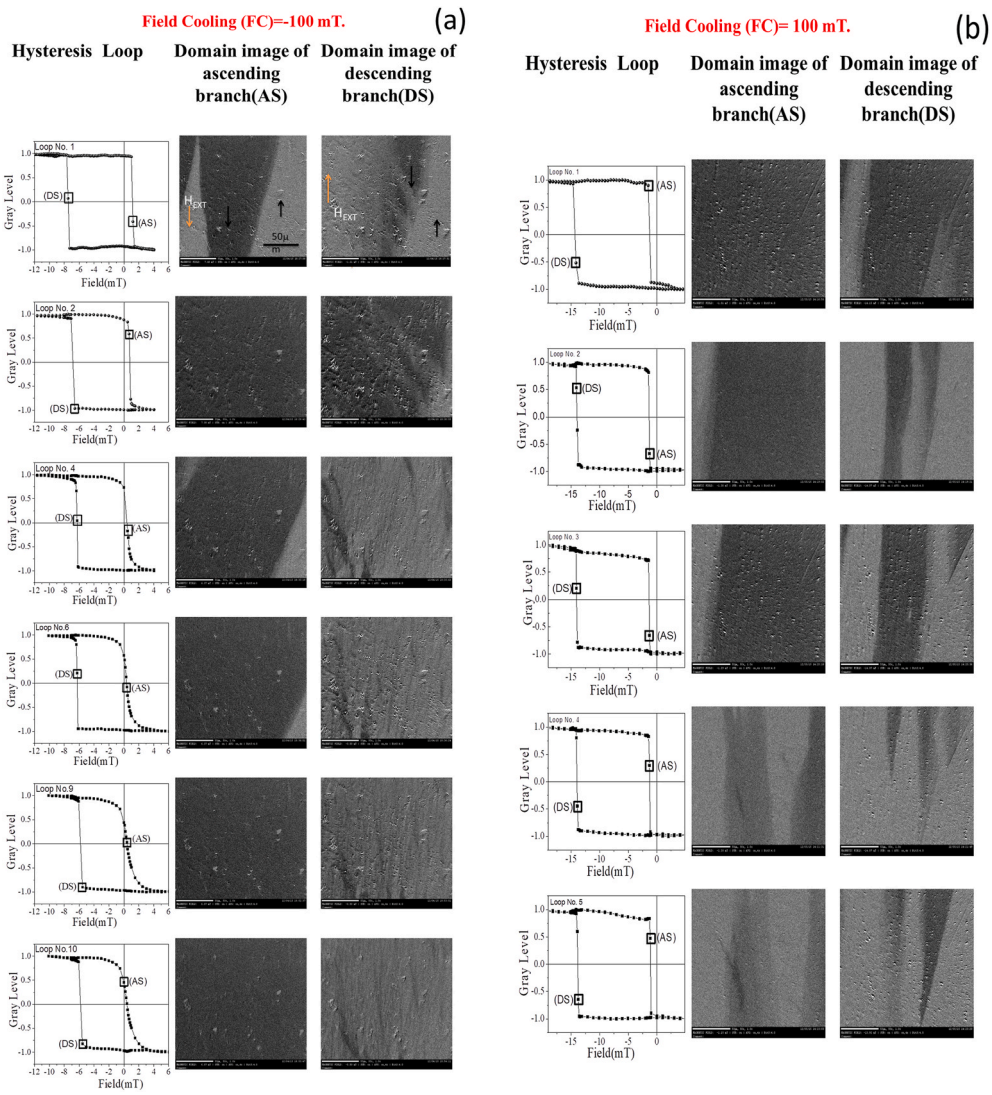

Fig. 3. M − H hysteresis loop with number of loops (n) along with domain images captures for the ion-irradiated specimens with the ion -fluence (a) 5×10^{16}ions/cm^2, (b) 1×10^{17}ions/cm^2 at 50 K for ascending(AS) and descending branches (DS) branches of the loop close to the coercivity.

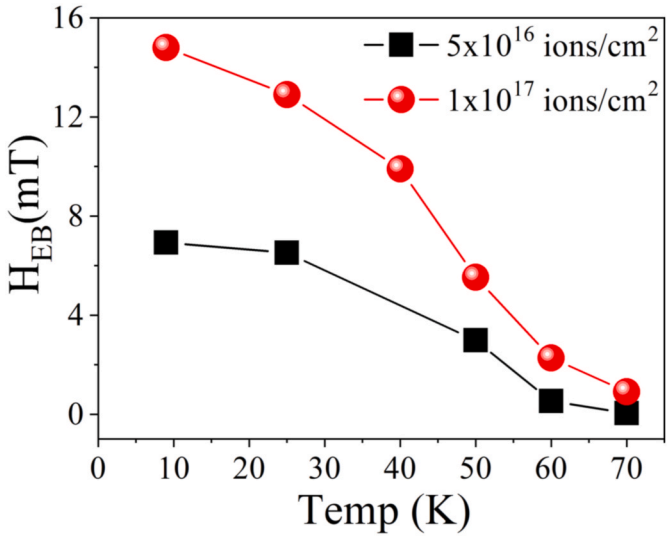

Fig. 4. Exchange bias value (H_{EB}) as a function of temperature for 5×10^{16} ions/cm^2 and 1×10^{17} ions/cm^2 of F-ion implanted specimens.

are given in Table 2.

4. Conclusions

The training effect and the evolution of the magnetic domain during the magnetization irreversible process have been studied at 50 K for F-ion implanted specimens. Magnetic irreversibility has been observed with training effect which is also confirmed by domain images from Kerr microscopy. The value of γ which is smaller for higher fluence specimen indicates a behavior that is changing from non-equilibrium state to equilibrium state. On the other hand, the increased value of C that is giving the information of the behavior of training effect is suggesting step-like behavior. For 1×10^{17} F-ions/cm^2 sample, change in the exchange bias field after measuring the 6th cycle is 4.42% while in case of 5×10^{16} F-ions/cm^2 is 27.32%. Remarkably, for the largest fluences, the relative training becomes smaller than the one for the low fluence that indicates suitability for device application. The temperature behavior of the H_{EB} value for both the ion-fluences are identical while the H_{EB} value for the specimen 1×10^{17} ions/cm^2 is much higher.

We have also investigated the temperature dependence of H_{EB} for both the specimens 5×10^{16} ions/cm^2 and 1×10^{17} ions/cm^2. The exchange bias field disappeared at ~70 K which is near to Néel temperature of FeF_2(T_N = 78 K) indicating anti-ferromagnetic anisotropy is

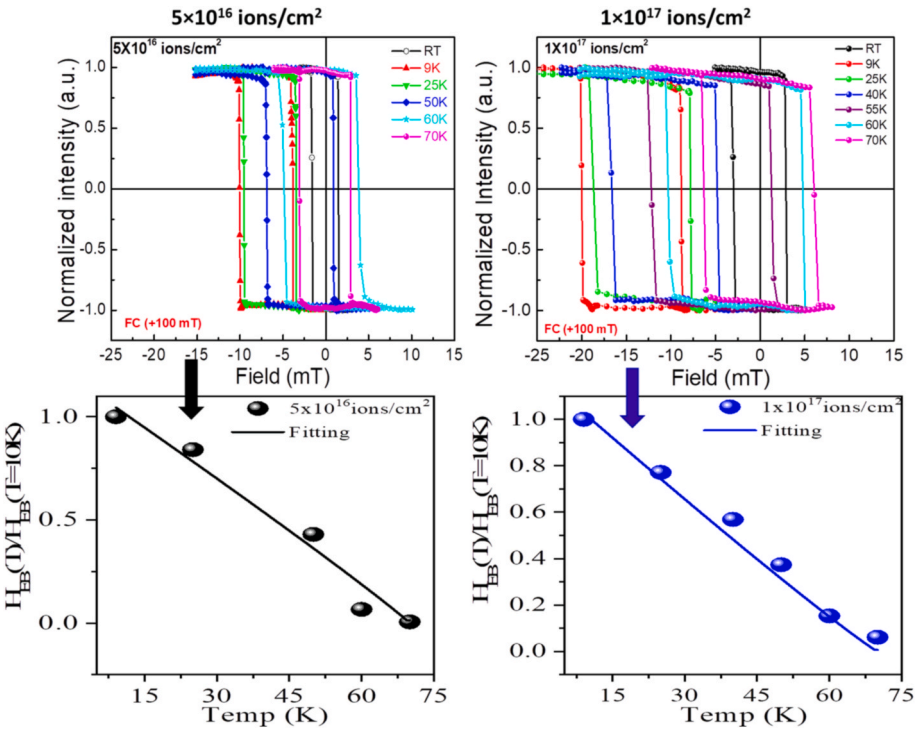

Fig. 5. (Left) Temperature-dependent M − H loops of 5×10^{16} ion/cm^2 after field cooling down to 10 K and corresponding results of best-fitting from Eq^n.5 similarly (Right) temperature-dependent M − H loops of 1×10^{17} ion/cm^2 and corresponding fitting with the same model.

Table 2
Fitting parameters for 5×10^{16} ions/cm^2 and 1×10^{17} ions/cm^2 sample according to Eq. (5).

Sample	B	ν
5×10^{16} ion/cm^2	0.84	1.15
1×10^{17} ion/cm^2	0.87	0.95

responsible for the exchange bias effect. $H_{EB}(T)$ variation is fitted within the Malozemoff model with a modified exponent. The value of ν is greatly reduced i.e., $\nu = 0.92$, for 1×10^{17} ion/cm^2 sample, indicating close to the cubic anisotropy of FeF_2 while in case of 5×10^{16} ion/cm^2 the value of ν is 1.12 which shifts from cubic anisotropy of AFM.

Credit authour statement

Dr, Sagar Sen did the experiment and analysis, Prof. Ajay Gupta did critical reading, modifications in the manuscript and scientific discussions with other authors. Dr. V.R. Reddy supervised the experiment and Prof. Ratnesh Gupta did concept design and paper writing.

Declaration of competing interest

The authors declare that they have no known competing financial interests or personal relationships that could have appeared to influence the work reported in this paper.

Acknowledgment

We thankful to Prof. H. Hofsaess, Univ. of Gottingen, Germany and D.Purschke for the fluorine ion implantation. Authors are thankful for financial support of the UGC-DAE-CSR, Indore and Inter-University Accelerator Centre, New Delhi.

References

[1] J. Nogués, I.K. Schuller, Exchange bias, J. Magn. Magn Mater. 192 (1999) 203–232, https://doi.org/10.1016/S0304-8853(98)00266-2.
[2] M. Ohkoshi, K. Tamari, M. Harada, S. Honda, T. Kusuda, Microstructure and exchange anisotropy of Co-CoO sputtered films with perpendicular magnetization, IEEE Translat J. Magn. Jpn. 1 (1985) 37–38, https://doi.org/10.1109/TJMJ.1985.4548441.
[3] C. Binek, A. Hochstrat, X. Chen, P. Borisov, W. Kleemann, B. Doudin, Electrically controlled exchange bias for spintronic applications, J. Appl. Phys. 97 (2005), 10C514, https://doi.org/10.1063/1.1853836.
[4] P. Grnberg, R. Schreiber, Y. Pang, M.B. Brodsky, H. Sowers, Layered magnetic structures: evidence for antiferromagnetic coupling of Fe layers across Cr interlayers, Phys. Rev. Lett. 57 (1986) 2442–2445, https://doi.org/10.1103/PhysRevLett.57.2442.
[5] M.N. Baibich, J.M. Broto, A. Fert, F.N. Van Dau, F. Petroff, P. Eitenne, G. Creuzet, A. Friederich, J. Chazelas, Giant magnetoresistance of (001)Fe/(001)Cr magnetic superlattices, Phys. Rev. Lett. 61 (1988) 2472–2475, https://doi.org/10.1103/PhysRevLett.61.2472.
[6] W.H. Meiklejohn, Exchange anisotropy - a review, J. Appl. Phys. 33 (1962) 1328–1335, https://doi.org/10.1063/1.1728716.
[7] D. Mauri, H.C. Siegmann, P.S. Bagus, E. Kay, Simple model for thin ferromagnetic films exchange coupled to an antiferromagnetic substrate, J. Appl. Phys. 62 (1987) 3047–3049, https://doi.org/10.1063/1.339367.
[8] A.P. Malozemoff, Random-field model of exchange anisotropy at rough ferromagnetic- antiferromagnetic interfaces, Phys. Rev. B 35 (1987) 3679–3682, https://doi.org/10.1103/PhysRevB.35.3679.
[9] J. Nogués, J. Sort, V. Langlais, V. Skumryev, S. Suriñach, J.S. Muñoz, M.D. Baró, Exchange bias in nanostructures, Phys. Rep. 422 (2005) 65–117, https://doi.org/10.1016/j.physrep.2005.08.004.
[10] R.L. Stamps, Mechanisms for exchange bias, J. Phys. D Appl. Phys. 33 (2000), R247, https://doi.org/10.1088/0022-3727/33/23/201.
[11] M. Gruyters, D. Riegel, Strong exchange bias by a single layer of independent antiferromagnetic grains: the CoO/Co model system, Phys. Rev. B 63 (2001), 052401, https://doi.org/10.1103/PhysRevB.63.052401.
[12] F. Radu, M. Etzkorn, T. Schmitte, R. Siebrecht, A. Schreyer, K. Westerholt, H. Zabel, Asymmetric magnetization reversal on exchange biased CoO/Co bilayers, J. Magn. Magn Mater. 240 (2002) 251–253.
[13] C. Binek, Training of the exchange-bias effect: a simple analytic approach, Phys. Rev. B 70 (2004), 014421, https://doi.org/10.1103/PhysRevB.70.014421.
[14] Y.X. Gao, C.M. Zhu, S. Huang, Z.M. Tian, S.L. Yuan, Size dependent training of exchange bias effect in CuFe2O4/CuO nanocomposites, J. Magn. Magn Mater. 439 (2017) 384–390, https://doi.org/10.1016/j.jmmm.2017.03.045.
[15] D. Paccard, C. Schlenker, O. Massenet, R. Montmory, A. Yelon, A new property of ferromagnetic-antiferromagnetic coupling, Phys. Status Solidi 16 (1966) 301–311, https://doi.org/10.1002/pssb.19660160131.

[16] L.E. Fernandez-Outon, G. Vallejo-Fernandez, S. Manzoor, K. O'Grady, Thermal instabilities in exchange biased materials, J. Magn. Magn Mater. 303 (2006) 296–301, https://doi.org/10.1016/j.jmmm.2006.01.080.
[17] A.G. Biternas, R.W. Chantrell, U. Nowak, Dependence of training effect on the antiferromagnetic structure of exchange-bias bilayers within the domain-state model, Phys. Rev. B 89 (2014), 184405, https://doi.org/10.1103/PhysRevB.89.184405.
[18] A.G. Biternas, R.W. Chantrell, U. Nowak, Behavior of the antiferromagnetic layer during training in exchange-biased bilayers within the domain state model, Phys. Rev. B 82 (2010), 134426, https://doi.org/10.1103/PhysRevB.82.134426.
[19] A.G. Biternas, U. Nowak, R.W. Chantrell, Training effect of exchange-bias bilayers within the domain state model, Phys. Rev. B Condens. Matter 80 (2009), 134419, https://doi.org/10.1103/PhysRevB.80.134419.
[20] S. Sen, B.K. Panigrahi, R.J. Choudhary, A. Gupta, R. Gupta, Evolution of magnetic anisotropy by O ion implantation in Fe/Co/Fe trilayar, Phys. B Condens. Matter 570 (2019) 241–245, https://doi.org/10.1016/j.physb.2019.06.036.
[21] M.G. Le Boité, A. Traverse, L. Névot, B. Pardo, J. Corno, Characterization of ion-beam mixed multilayers via grazing x-ray reflectometry, J. Mater. Res. 3 (1988) 1089–1096, https://doi.org/10.1557/JMR.1988.1089.
[22] S. Balaji, B.K. Panigrahi, S. Amirthapandian, S. Kalavathi, A. Gupta, K.G.M. Nair, The mechanism of phase formation in Pt/Co bilayers during ion beam mixing, Nucl. Instrum. Methods B 313 (2013) 60–63, https://doi.org/10.1016/j.nimb.2013.08.005.
[23] J. Ziegler, URL (http://www.srim.org/).
[24] S.R. Ali, M.R. Ghadimi, M. Fecioru-Morariu, B. Beschoten, G. Güntherodt, Training effect of the exchange bias in Co/CoO bilayers originates from the irreversible thermoremanent magnetization of the magnetically diluted antiferromagnet, Phys. Rev. B 85 (2012), 012404, https://doi.org/10.1103/PhysRevB.85.012404.
[25] Z. Hussain, V. Raghavendra Reddy, Kerr microscopy study of thermal and athermal training effects in a Co/CoO exchange bias system, J. Appl. Phys. 122 (2017), https://doi.org/10.1063/1.4986415, 0–7.
[26] S. Polisetty, S. Sahoo, C. Binek, Scaling behavior of the exchange-bias training effect, Phys. Rev. B 76 (2007), 184423, https://doi.org/10.1103/PhysRevB.76.184423.
[27] N.N. Phuoc, T. Suzuki, Mechanism of Blocking Temperature Difference for Parallel and Perpendicular Exchange Biases in FePt/FeMn Multilayers, IEEE Trans. Magn., 2007, pp. 897–899, https://doi.org/10.1109/TMAG.2006.888498.
[28] W. Zhang, D.N. Weiss, K.M. Krishnan, Competing anisotropies and temperature dependence of exchange bias in Co|IrMn metallic wire arrays fabricated by nanoimprint lithography, J. Appl. Phys. 107 (2010), 1413, https://doi.org/10.1063/1.3367959.